Research Paper

Spatial scaling of urban impervious surfaces across evolving landscapes: From cities to urban regions

Qun Ma[a], Jianguo Wu[b,a,*], Chunyang He[a,*], Guohua Hu[c]

[a] Center for Human-Environment System Sustainability (CHESS), State Key Laboratory of Earth Surface Processes and Resource Ecology (ESPRE), Faculty of Geographical Science, Beijing Normal University, Beijing 100875, China
[b] School of Life Sciences, School of Sustainability, and Julie Ann Wrigley Global Institute of Sustainability, Arizona State University, Tempe, AZ 85287, USA
[c] Key Lab of Geographic Information Science (Ministry of Education), School of Geographic Sciences, East China Normal University, Shanghai 200241, China

A B S T R A C T

Urban impervious surfaces (UIS) influence the structure and function of urban systems, and are widely considered a key indicator of urban environmental conditions. However, the amount and pattern of UIS both change with spatial scale, which complicates the computation and interpretation of UIS as an indicator. A better understanding of the spatial scaling relations of UIS is needed to resolve this predicament. Thus, the main objective of this study was to explore how UIS would change with increasing spatial extent and population size across urban hierarchical levels, using data from the three largest urban agglomerations in China. In addition, a comparative analysis of six world metropolitan regions was conducted to test the generality of the UIS scaling relations. Scalograms and standardized major axis regression were used to investigate the scaling relations with respect to spatial extent and city size, respectively. Our major findings include: (1) the total amount of UIS increased, whereas the percentage of UIS decreased, in a staircase-like fashion when the spatial extent of analysis expanded from within a local city to the entire urban agglomeration; (2) the spatial scaling of UIS followed a rather consistent and tight power law function within a local city, but became less consistent and less tight beyond a local city; (3) the scaling relations of the total amount of UIS were more consistent than those of the percentage of UIS, and the total amount of UIS scaled more tightly with urban area than with urban population size. These findings shed new light on the scale dependence of UIS, suggesting that a multiscale approach should be adopted for quantifying UIS and for using it as an urban environmental indicator.

1. Introduction

Urbanization worldwide has converted more and more natural and agricultural lands into urban impervious surfaces (UIS) – i.e., human-made land covers in urban areas through which water cannot penetrate, including rooftops, roads, driveways, sidewalks, and parking lots (Arnold & Gibbons, 1996; Ma, He, & Wu, 2016; Ma, Wu, & He, 2016; Weng, 2012). In 2010, the global total of UIS was about 0.6 million km^2 (or 0.45% of the global land area excluding Antarctica and Greenland), and it has continued to increase rapidly (Liu, He, & Wu, 2016; Liu, He, Zhou, & Wu, 2014; Zhou et al., 2015). For example, the total amount of UIS of mainland China was 10,614.23 km^2 in 1992, and increased to 31,147.63 km^2 in 2009, tripling within 17 years (Ma et al., 2014).

While UIS occupies relatively a small portion of the land area on a regional or global scale, its myriad environmental impacts are disproportionately large (Arnold & Gibbons, 1996; Forman, 2016; Grimm et al., 2008; Luck, Jenerette, Wu, & Grimm, 2001). UIS can change the land surface energy balance, resulting in urban heat islands (Buyantuyev & Wu, 2010; Ma, Wu et al., 2016; Oke, 1982); increase the volume and intensity of urban runoff, leading to urban flooding (Brun & Band, 2000; Weng, 2001); and reduce water quality, degrading aquatic biodiversity and wetland ecosystems (Brabec, 2002; Goetz & Fiske, 2008). Thus, impervious surface coverage is not only a major measure of urbanization itself, but also a key indicator of environmental conditions (Arnold & Gibbons, 1996; Wu, 2014).

Thus, it is important to quantify the amount and spatial distribution of UIS for better understanding urbanization patterns and their environmental consequences. Towards this end, much work has been done during the past few decades based on remote sensing data (Elvidge et al., 2007; Lu, Li, Kuang, & Moran, 2014; Ma et al., 2014; Ma,

Wu et al., 2016). However, while we know that urban systems are hierarchically structured, in which large urban regions are composed of smaller sub-regions which in turn comprise individual cities (Batty, 2008; Li, Li, & Wu, 2013; Wu, 1999; Wu & David, 2002), little research has been done to quantify how UIS changes with spatial scale along the hierarchy of administrative levels. Yet, knowing how UIS is structured spatially from the local city to the regional urban agglomeration – i.e., the spatial scaling of UIS – is essential for understanding the patterns and processes of urbanization as well as their environmental impacts on multiple scales.

Quantifying the spatial pattern of UIS necessarily requires a multi-scale approach, and scaling relations need to be developed for describing multiscale patterns and making predictions across scales, as numerous studies in ecological and geographical sciences have shown that spatial pattern is scale-dependent (Jelinski & Wu, 1996; Levin, 1992; Liu et al., 2016; Saura, 2004; Shen, Darrel Jenerette, Wu, & Gardner, 2004; Wu, 2004; Wu, Shen, Sun, & Tueller, 2002). Scaling usually refers to the translation of information across spatial and temporal scales or organizational levels, which frequently involves changing grain size, extent, or both (Wiens, 1989; Wu, 1999; Wu, Bruce Jones, Li, & Loucks, 2006). Wu et al. (2002) and Wu (2004) systematically examined the scaling relations of commonly used landscape metrics with respect to changing grain size and extent, and identified three general categories: simple scaling functions (linear or power laws), staircase-like functions, and unpredictable behavior. These findings have consequently been confirmed and amended by several studies (Argañaraz & Entraigas, 2014; Frazier, 2016; Frohn & Hao, 2006; Saura & Castro, 2007; Shen et al., 2004). These scaling relations are informative for understanding the multiscale structural properties of landscapes, and allow for cross-scale predictions when they can be expressed as mathematical functions (Wu, 2004; Wu et al., 2002).

Do such scaling relations exist for UIS when we measure them from a local city to its surrounding urban region and the even greater urban agglomeration? To address this question, we systematically examined the spatial scaling of UIS with respect to changing extent in three major urban megaregions of China, and then we further tested the generality of the UIS scaling relations by conducting similar analyses with several major metropolitan regions around the world. The study was designed to address the following questions: How does UIS change with increasing spatial extent across the administrative levels of urban hierarchy? How do the total amount and percentage of UIS scale differently in space? How does the scaling of UIS in space compare with the scaling of UIS with respect to urban population? Do the scaling relations of UIS derived from Chinese metropolitan regions apply to the world's other metropolitan regions?

2. Methods

2.1. Study area

China, as one of the fastest urbanizing nations around the world, has experienced a rapid and large-scale expansion of UIS, with an annual growth rate of 6.54% since 1992 (Ma et al., 2014). As the urban growth rate continues to accelerate in terms of both urbanized land area and urban human population, a number of urban agglomerations with different levels of economic and social development have emerged across China (Fang, 2011; Fang, 2015; Wu, Xiang, & Zhao, 2014). The three largest national-level urban agglomerations are the Beijing-Tianjin-Hebei (BTH) urban agglomeration, the Yangtze River Delta (YRD) urban agglomeration, and the Pearl River Delta (PRD) urban agglomeration. These three urban agglomerations together account for nearly 40% of the total UIS area, 36% of gross domestic product, and 18% of the total population of China (Ma et al., 2014; State Council of the People's Republic of China, 2014). We chose BTH, YRD, and PRD as the focal sites of our study (Fig. 1) because of their extraordinary environmental and socioeconomic importance, as well as their complete

urban hierarchy that extends from the local city to the much broader region of urban agglomeration. In addition, these three urban agglomerations are not only the largest in China, but also have contrasting spatial patterns and urbanization trends due to different population densities and socioeconomic conditions (Kuang, Chi, Lu, & Dou, 2014). All the above characteristics facilitate an in-depth analysis of the spatial scaling of UIS.

We delineated the boundary of each urban agglomeration based on Fang (2011), and derived the demographic and economic data described below from the Department of Urban Surveys of National Bureau of Statistics of China (2011) and the Population Census Office under the State Council and Employment Statistics of National Bureau of Statistics of China (2013). The BTH is located in the North Plain-eastern coastal region of China, with a total land area of 182,000 km². In 2010, the total population of this region reached 83.79 million with an urbanization level of 59.95%, and its total GDP exceeded 3776 billion CNY. The YRD lies in the eastern coastal region of China, covering an area of 107,500 km². The total population in 2010 was 106.51 million with an urbanization level of 69.75%, and the total GDP was 7591 billion CNY. The PRD is distributed in the southern coastal region of China, covering an area of 54,100 km². In 2010, the PRD had 56.13 million people and an urbanization level of 82.72%, and its total GDP exceeded 3700 billion CNY.

Our analysis followed a hierarchical approach to urban studies (Li et al., 2013; Ma, Wu et al., 2016; Wu, 1999; Wu & David, 2002), explicitly considering three administrative levels within each urban agglomeration (Fig. 1): the city proper, the metropolitan region, and the urban agglomeration as a whole. The three levels formed a spatially nested urban landscape hierarchy as each city proper belonged exclusively to a metropolitan region which in turn was part of an urban agglomeration. Specifically, the BTH, YRD, and PRD each contained a megacity (the Beijing metropolitan region, the Shanghai metropolitan region, and the Guangzhou metropolitan region, respectively) whose city proper was chosen as the lowest level of analysis (Fig. 1).

2.2. Data acquisition and processing

The UIS map of China in 2009 with a spatial resolution of 1 × 1 km (Ma et al., 2014) was used in this study. In an earlier study, we developed an improved way of mapping UIS for large regions and quantified the UIS dynamics of China from 1992 to 2009 (Ma et al., 2014). The study utilized four types of remote sensing data to estimate the UIS of China in 2009: the Defense Meteorological Satellite Program's Operational Linescan System (DMSP/OLS) nighttime light (NTL) data (http://ngdc.noaa.gov/eog/dmsp/downloadV4composites.html), the Moderate Resolution Imaging Spectroradiometer (MODIS) 16-day Normalized Difference Vegetation Index (NDVI) composite data (https://ladsweb.nascom.nasa.gov/search/), high-resolution images available on Google Earth, and land use/cover data (http://www.geodata.cn/). The NTL data given in 30-arc-second grids and the annual mean NDVI data derived from the MODIS 16-day 1-km NDVI composite data in 2009 were projected onto an Albers Conical Equal Area Projection and resampled to a pixel size of 1 km based on a nearest neighbor resampling algorithm. The land use/cover data of China for 2010 were used as the reference data for extracting urban areas in 2009. Urban areas in this study refer to places with intensive human activities and extensive human-made land covers that include urban impervious surfaces, parks, and swimming pools/artificial ponds (Potere & Schneider, 2007; Wang et al., 2012). Detailed information on how these urban areas were classified is found in Ma et al. (2014). The accuracy assessment showed that our results of China's UIS had a much higher accuracy than previous estimates using NTL data, with the average root-mean-square error (RMSE) of 0.128, mean absolute error (MAE) of 0.105, systematic error (SE) of −0.008, and correlation coefficient (R) of 0.846 in 2009 (Ma et al., 2014). More details on the acquisition and processing of remote sensing data and estimation of UIS
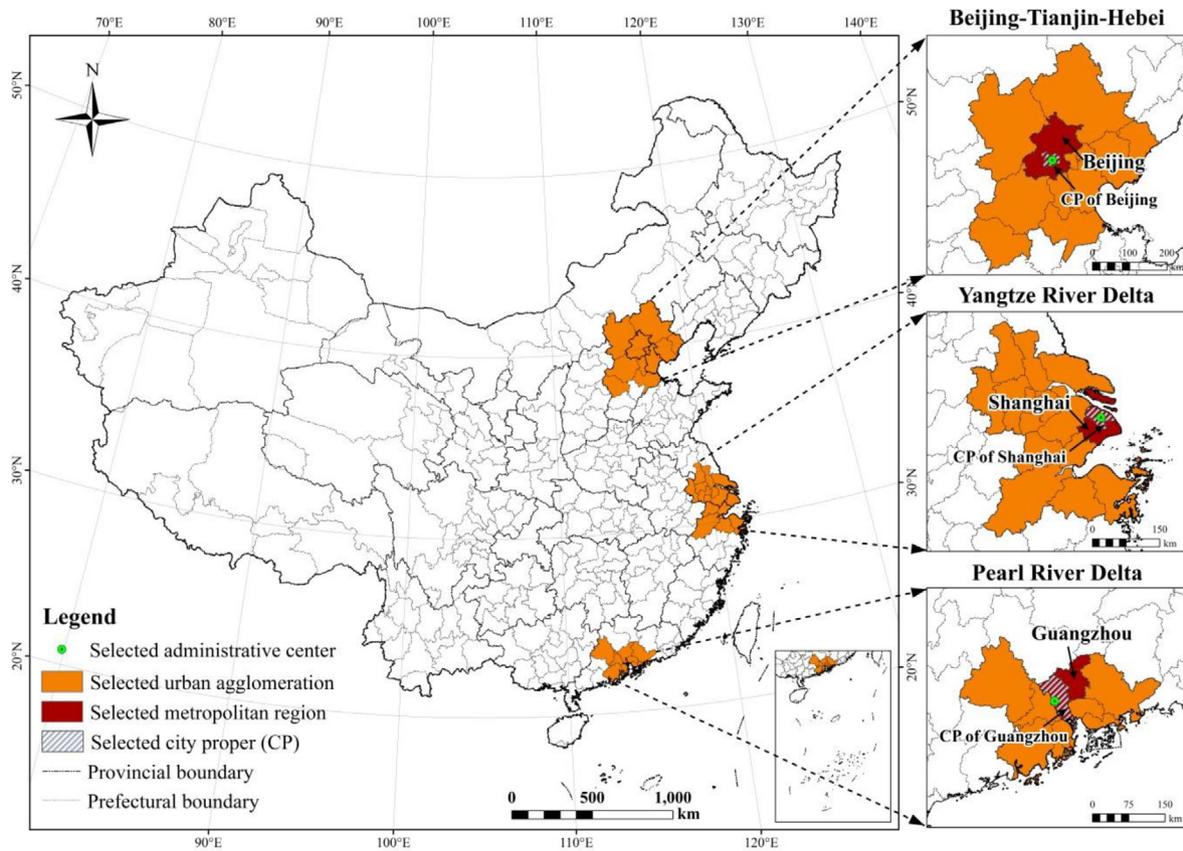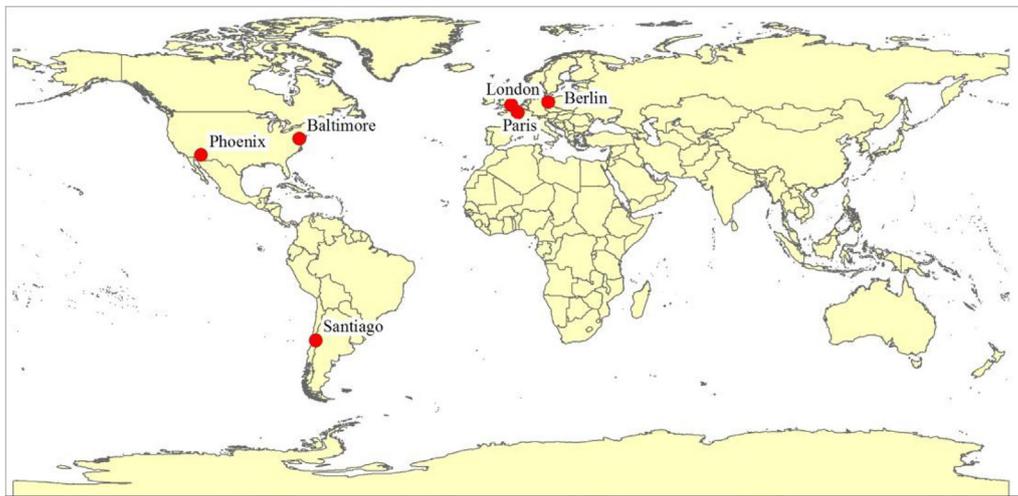
(a)
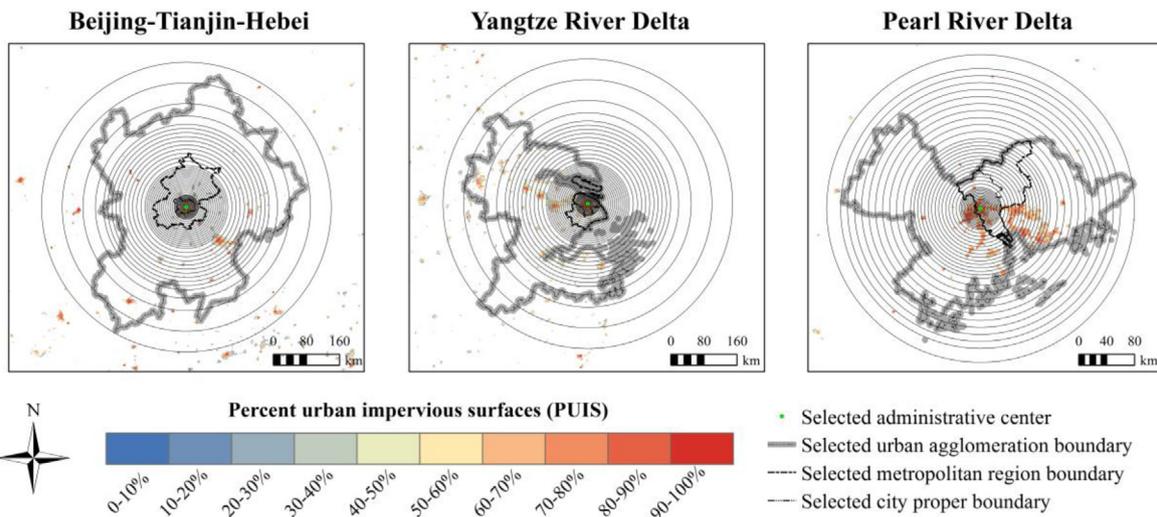
(b)

Fig. 1. Locational map of the three major urban agglomerations of China (a) and a schematic illustration of the concentric circle approach to changing spatial extent in the three main urban agglomerations of China (b). The three major urban agglomerations of China include the Beijing-Tianjin-Hebei urban agglomeration, the Yangtze River Delta urban agglomeration, and the Pearl River Delta urban agglomeration. Three levels of the administrative hierarchy are identified explicitly within each urban agglomeration: the city proper, the metropolitan region, and the urban agglomeration as a whole.

can be found in Ma et al. (2014).

LandScan population data in 2010 were obtained from the Oak Ridge National Laboratory (ORNL) (http://web.ornl.gov/sci/landscan/landscan_data_avail.shtml). The data are 30 arc seconds grids, covering −180 to 180 degrees in longitude and −90 to 84 degrees in latitude. The values of the grids are integer population counts, representing an

ambient population distribution (average over 24 h). The ambient population distribution integrates diurnal movements and collective travel habits of people into a single measure, and thus is a population distribution in totality, not just in terms of the locations where people live (Dobson, Bright, Coleman, Durfee, & Worley, 2000). We projected the data onto an Albers Conical Equal Area projection and resampled

(a)

Phoenix **Baltimore** **Santiago**

London **Paris** **Berlin**

Percent urban impervious surfaces (PUIS)

0-10% 10-20% 20-30% 30-40% 40-50% 50-60% 60-70% 70-80% 80-90% 90-100%

Locations of the selected world metropolitan regions

Selected metropolitan region boundary

National boundary
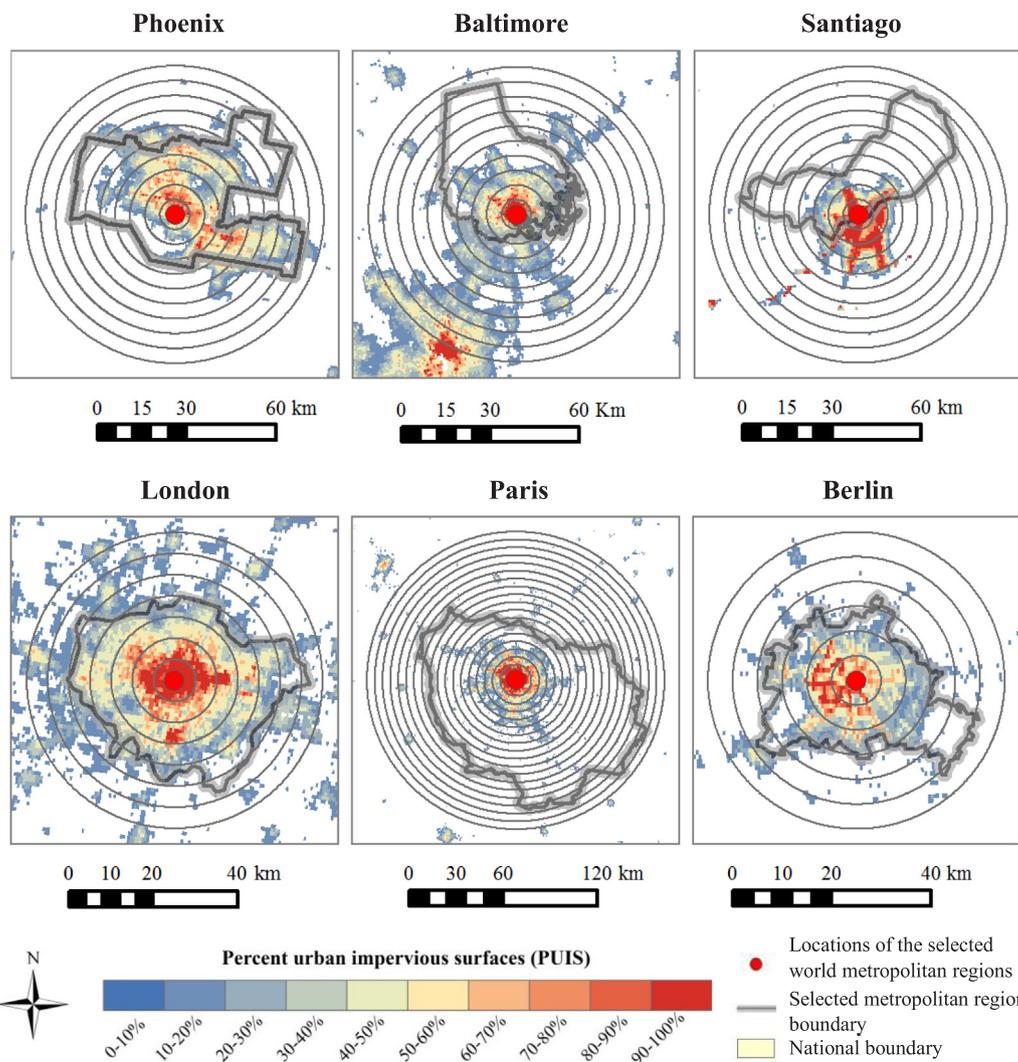
(b)

Fig. 2. Locational map of six world metropolitan regions: Phoenix of USA, Baltimore of USA, Santiago of Chile, London of England, Paris of France, and Berlin of Germany (a), with an illustration of increasing spatial extent with the concentric circle approach (b).

the data to a pixel size of 1 km based on a nearest neighbor resampling algorithm. The population counts in urban areas were extracted for each urban agglomeration. The boundaries of administrative units were based on the National Geomatics Center of China at the scale of 1: 4,000,000.

For examining the generality of our findings from Chinese

metropolitan regions, we selected six well-known metropolitan regions from other parts of the world: the Baltimore metropolitan region and the Phoenix metropolitan region in the United States, the Santiago metropolitan region in Chile, the London metropolitan region in the United Kingdom, the Paris metropolitan region in France, and the Berlin metropolitan region in Germany (Fig. 2a). The six world metropolitan regions were chosen because of their high urbanization levels and different urban development patterns, as well as their geographic representativeness (two regions in North America, three regions in Europe, and one region in South America). The impervious surfaces area data in 2010 for all the six metropolitan regions were obtained from the National Oceanic and Atmospheric Administration (NOAA)/ National Center for Environmental Information (NCEI) website (https://ngdc.noaa.gov/eog/dmsp/download_global_isa.html). The same hierarchical approach was used in analyzing these six world metropolitan regions (Fig. 2b).

2.3. Quantifying UIS scaling relations with respect to spatial extent

We adopted the scalogram approach (Wu, 2004; Wu et al., 2002) to quantify the effects of changing spatial extent on UIS across urban administrative levels, using a series of concentric circles with increasing radii (Fig. 1b; Table 1). The origin of concentric circles was located at the administrative center of the selected metropolitan region in each urban agglomeration (Fig. 1b). The spatial extent was represented by the total area of a concentric circle, within which the amount of UIS was calculated. Then scalograms were constructed by plotting the total area and percentage of UIS against the spatial extent (i.e., incrementally larger concentric circles across the three urban administrative levels).

2.4. Quantifying UIS scaling relations with respect to urban population and urban area

The power law scaling relation is usually expressed as: $Y = aX^b$. In the case of spatial scaling or spatial allometry (Wu & Li, 2006), Y is a variable of interest, X is the spatial scale (grain size or extent), a is the normalization constant, and b is the scaling exponent (i.e., the slope of the straight line in a log-log plot). If $b = 1$, Y and X have a simple linear relationship (called isometric scaling), meaning that Y changes with X proportionally. If $b \neq 1$, then the relationship is called allometric scaling (Wu & Li, 2006). In this study, we used standardized major axis (SMA) regression to examine if power-law scaling relations exist

Table 1
List of the radii of concentric circles used in the study at different urban administrative levels for the three key urban agglomerations of China. The largest spatial extent for each administrative level corresponds to the area of the concentric circle just large enough to enclose the whole urban region for the corresponding level.

Changing the radii of concentric circles (km)								
CP of Beijing	Beijing	BTH	CP of Shanghai	Shanghai	YRD	CP of Guangzhou	Guangzhou	PRD
4	4	4	4	4	4	4	4	4
6	6	6	6	6	6	6	6	6
8	8	8	8	8	8	8	8	8
10	10	10	10	10	10	10	10	10
12	12	12	12	12	12	12	12	12
14	14	14	14	14	14	14	14	14
16	16	16	16	16	16	16	16	16
18	18	18	18	18	18	18	18	18
20	20	20	20	20	20	20	20	20
22	22	22	22	22	22	22	22	22
24	24	24	24	24	24	24	24	24
26	26	26	26	26	26	26	26	26
28	28	28	28	28	28	28	28	28
30	30	30	30	30	30	30	30	30
	35	35	35	35	35	35	35	35
	40	40	40	40	40	40	40	40
	45	45		45	45	45	45	45
	50	50		50	50	50	50	50
	55	55		55	55	55	55	55
	60	60		60	60	60	60	60
	65	65		65	65	65	65	65
	70	70		70	70	70	70	70
	75	75			75		75	75
	80	80			80		80	80
	85	85			85		85	85
	90	90			90		90	90
	95	95			95		95	95
	100	100			100		100	100
	110	110			110		110	110
	120	120			120		120	120
	130	130			130			130
					140			140
					150			150
					160			160
					170			170
					180			180
					190			190
					200			200
					220			220
					250			
					300			
					350			

Note: CP represents the city proper, BTH represents the Beijing-Tianjin-Hebei urban agglomeration, YRD represents the Yangtze River Delta urban agglomeration, and PRD represents the Pearl River Delta urban agglomeration.

between the UIS measures (*Y*) and spatial extent or urban population size (*X*).

The SMA regression is a least-squares method with the purpose of not predicting one variable from another variable as linear regression aims to do, but describing how two variables are related, typically as a linear relationship on logarithmic scales (Warton, Wright, Falster, & Westoby, 2006). Thus, the SMA regression can be used to test if a power law-like relationship (e.g., an allometric relation) is supported by data, and to determine what the specific value of the scaling exponent is. By contrast, the ordinary least squares (OLS) regression is generally used to test for an association between *Y* and *X* and to predict *Y* from *X* through estimating the line which is fitted to minimize the sum of squares of residuals measured in the *Y* axis (Warton et al., 2006). The purpose of this study was not to test for a correlation between UIS, urban area, and urban population, but to investigate if power law-like relationships exist between them and to compare slopes for their relationships. In this case, the SMA regression is more appropriate than the OLS regression (Fuller & Gaston, 2009; Li, Han, & Wu, 2006).

We first calculated the total area of UIS, urban population size (i.e., the total ambient population in urban areas), and urban area, and then conducted SMA regression analysis to derive the scaling relations of UIS with respect to increasing urban population and urban area, respectively. Confidence intervals for the estimated scaling exponent (*b*) were computed, with one-sample tests of scaling exponent with a null hypothesis $b = 1$. All statistical analyses were performed with SMATR Version 2.0.

3. Results

3.1. Scaling relations of UIS with respect to changing spatial extent

As mentioned earlier, we chose both the total area and percentage of UIS to explore how UIS scales with spatial extent across urban administrative levels (the city proper, the metropolitan region, and the urban agglomeration). In this section, we organized our results according to these administrative levels and the two UIS measures (the total area and percentage).

3.1.1. Scaling relations of the total area of UIS

Within a city proper, as the spatial extent (represented by the areas of concentric circles) increased, the total area of UIS for the three cities proper all followed a power law with a scaling exponent of between 0 and 1 (Fig. 3a-c). Within a metropolitan region, as the spatial extent increased beyond the city proper level, the total area of UIS continued to increase, but at a slower rate (Fig. 3d-f). As the spatial extent further increased beyond the metropolitan region, the scalograms of the total area of UIS showed an upward staircase-like curve for the three urban agglomerations (Fig. 3g-i). The total area of UIS continued to increase rapidly beyond the metropolitan region for the BTH and YRD urban agglomerations (Fig. 3g, h), but ceased to increase for the PRD urban agglomeration (Fig. 3i).

3.1.2. Scaling relations of the percentage of UIS

Within a city proper, the percentage of UIS decreased linearly with increasing spatial extent (again represented by the areas of concentric circles) for the city proper of Beijing (Fig. 4a), followed a power law with a scaling exponent of between −1 and 0 for the city proper of Shanghai, and showed a downward staircase-like curve (with two segments of linear change) for the city proper of Guangzhou (Fig. 4c). As the spatial extent further increased to cover the entire metropolitan region, the percentage of UIS continued to decrease, but at a slower rate (Fig. 4d-f). Further increasing the spatial extent from the metropolitan region to the urban agglomeration resulted in little change in the percentage of UIS for all the three metropolitan regions (Fig. 4g-i).

While the general pattern of the scalograms for the three urban agglomerations looked similar, the details actually varied among them.

Moving from the city proper level to the urban agglomeration level, the YRD urban agglomeration (Fig. 4h) showed the largest drop in the percentage of UIS whereas the PRD urban agglomeration (Fig. 4i) exhibited the least. The percentage of UIS in the BTH urban agglomeration decreased rapidly first, then stayed relatively unchanged, and then increased slightly (Fig. 4g). The scalograms of the percentage of UIS (Fig. 4) mirrored, to some degrees, those of the total area of UIS (Fig. 3), but differences between them were visually apparent.

3.1.3. Comparison of UIS scaling relations between Chinese and other world metropolitan regions

The log-log scalograms of the six selected world metropolitan regions showed a general pattern quite similar to those of the Chinese metropolitan regions (comparing Figs. 5 and 6): with increasing spatial extent of analysis from the city center, increases in the total area of UIS were fast and linear (or following a power law) at first, then slowed down (e.g., Shanghai), and then picked up again (e.g., Beijing) or stayed relatively unchanged (e.g., Guangzhou). Specifically, the scalograms of Berlin and Paris closely resembled that of Beijing; the scalograms of Baltimore and London looked like that of Shanghai; and the scalograms of Phoenix and Santiago were similar to that of Guangzhou (Fig. 6). All scalograms exhibited scale breaks corresponding roughly to the boundaries of urban administrative levels (Figs. 5 and 6). Scale breaks are visualized more readily in a log-log plot in which a straight line represents a power law scaling (Wu et al., 2006).

3.2. Scaling relations of UIS with respect to urban population and urban area

For all the three major urban agglomerations of China, the total area of UIS increased with urban population size and urban area following a power-law function (Fig. 7; Table 2). All the power-law scaling relations were statistically significant, with P-values of smaller than 0.001 and R^2 ranging from 0.755 to 0.954 (Fig. 7; Table 2). The values of the scaling exponent varied greatly between the urban population- and urban area-based scaling relations. In the scaling relation between the total area of UIS and urban population size, the values of the scaling exponent were all smaller than 1 (i.e., 0.728 for BTH, 0.721 for YRD, and 0.809 for PRD). However, the values of the scaling exponent in the scaling relation between the total area of UIS and urban area were all larger than 1 (i.e., 1.139 for BTH, 1.116 for YRD, and 1.103 for PRD).

4. Discussion

4.1. How does UIS change with increasing spatial extent across the urban administrative hierarchy?

The major objective of this study was to quantify how UIS changes with increasing spatial extent across the three major administrative levels of urban hierarchy – the city proper, the metropolitan region, and the urban agglomeration. Our results show that, in general, the total area of UIS increased and the percentage of UIS decreased with increasing spatial extent, and the scaling relations varied across the three hierarchical administrative levels (Figs. 3–5). Within the city proper and between administrative levels of urban hierarchy, the spatial scaling relation was a power law (including the linear function as a special case of a power law with the scaling exponent being one). The scalograms of the city proper-metropolitan region-urban agglomeration hierarchy, however, exhibited a staircase-like pattern. The turning points where scaling relations change relatively abruptly in a scalogram represent scale breaks (Wu, 1999; Wu et al., 2006). These scale breaks in the spatial scaling relations of UIS found in our study corresponded largely to the administrative boundaries or the urban hierarchical levels (Figs. S1 and S2). At the same time, these scale breaks also roughly corresponded to the locations of multiple centers for each urban agglomeration. For example, the approximate locations of other centers
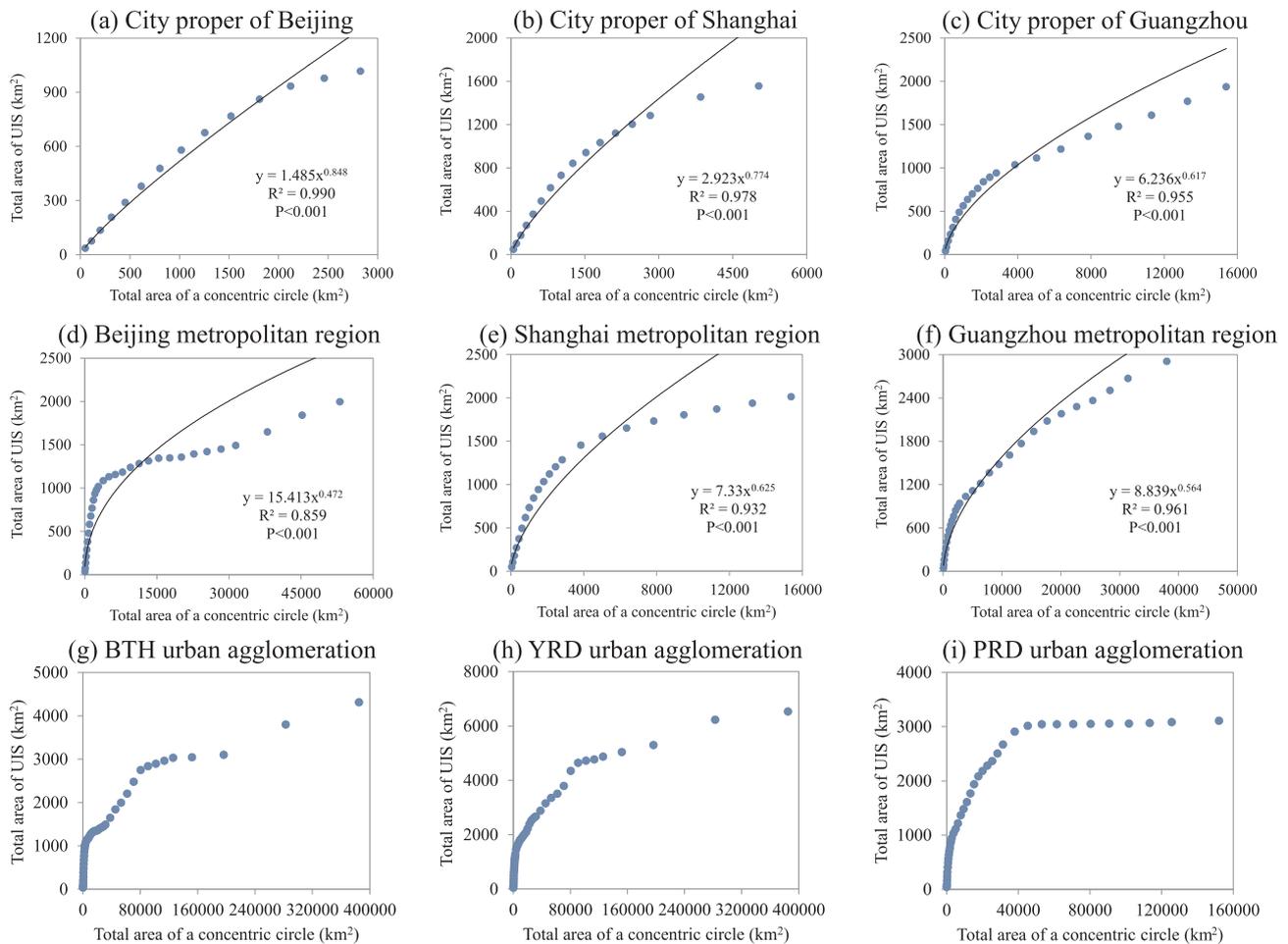
Fig. 3. Scalograms of the total area of urban impervious surfaces with respect to increasing spatial extent of analysis (represented as the areas of concentric circles) in three major megalopolitan regions of China at the three urban administrative levels: the city proper (a-c), the metropolitan region (d-f), and the urban agglomeration (g-i).

(e.g., Tianjin, Tangshan, and Shijiazhuang) of the BTH urban agglomeration were identified by the scalogram approach, which corresponded to the three scale breaks (Fig. S3). These results demonstrated that spatial scalograms were able to effectively identify the multiple scales across a broad urban region with multiple urban centers (Wu, 2004; Wu, Gao, & Tueller, 1997; Wu, Jelinski, Luck, & Tueller, 2000; Wu et al., 2002). These results corroborate the "scaling ladder" theory, which was based on hierarchy theory and spatial patch dynamics (Wu, 1999; Wu & David, 2002).

Why do UIS scaling relations exhibit a staircase-like pattern with several scale breaks across the three major administrative levels of urban hierarchy? Our previous study showed that major influencing factors for the spatiotemporal patterns of UIS in China varied substantially across hierarchical administrative levels, with demographic factors (e.g., urban population) dominating at the county level (Ma, He et al., 2016). The city-proper level in this study corresponded roughly to the county level, and thus demographic factors may contribute to the power-law scaling of UIS within this scale domain. Taking the city proper of Beijing as an example, it accounted for only 8.34% of Beijing's land area, but made up nearly 60% of the total population in Beijing for the year of 2010 (Beijing Municipal Bureau of Statistics NBS Survey Office in Beijing, 2011). High population densities seemed to play an important role in shaping the spatial pattern of UIS within the city proper. However, as the spatial extent increased beyond the city proper level, population densities declined markedly, resulting in the first staircase-like pattern of UIS and the occurrence of a scale break (Fig. S1a). As the spatial extent further increased beyond the Beijing metropolitan region, other metropolitan regions (e.g., Tianjin) with large

populations and extensive UIS were incorporated, leading to another staircase or scale break (Fig. S3). Overall, the spatial patterns of UIS were determined by a suite of demographic, economic, and traffic factors, as well as environmental settings, across scales (Ma, He et al., 2016).

4.2. Do the spatial scaling relations of UIS derived from Chinese metropolitan regions apply to metropolitan regions in other countries?

Or, do UIS scaling relations transcend national and continental boundaries? Our results show that two metropolitan regions in North America (i.e., Phoenix and Baltimore), three metropolitan regions in Europe (i.e., London, Paris, and Berlin), and one metropolitan region in South America (i.e., Santiago) all exhibited spatial scaling relations similar to those of the Chinese metropolitan regions (Figs. 5 and 6). Within the city proper, the total area of UIS increased quickly and in a power law-like fashion. But beyond the local city scale, the spatial scaling relations of UIS showed three somewhat different kinds of patterns: (1) UIS stayed relatively unchanged for Guangzhou, Phoenix, and Santiago; (2) UIS kept increasing at a slower rate for Shanghai, Baltimore, and London; and (3) the increase in UIS slowed down and then sped up again for Beijing, Paris, and Berlin (Figs. 5 and 6).

The differences in scaling pattern over broader spatial scales beyond the local city are reflective of the multiscaled configurations of metropolitan regions and urban agglomerations. If an urban region has multiple urban centers that are close to each other, the spatial scaling pattern would be of the first type (e.g., Guangzhou). In this case, most of UIS are located in a relatively small spatial extent, and the total area
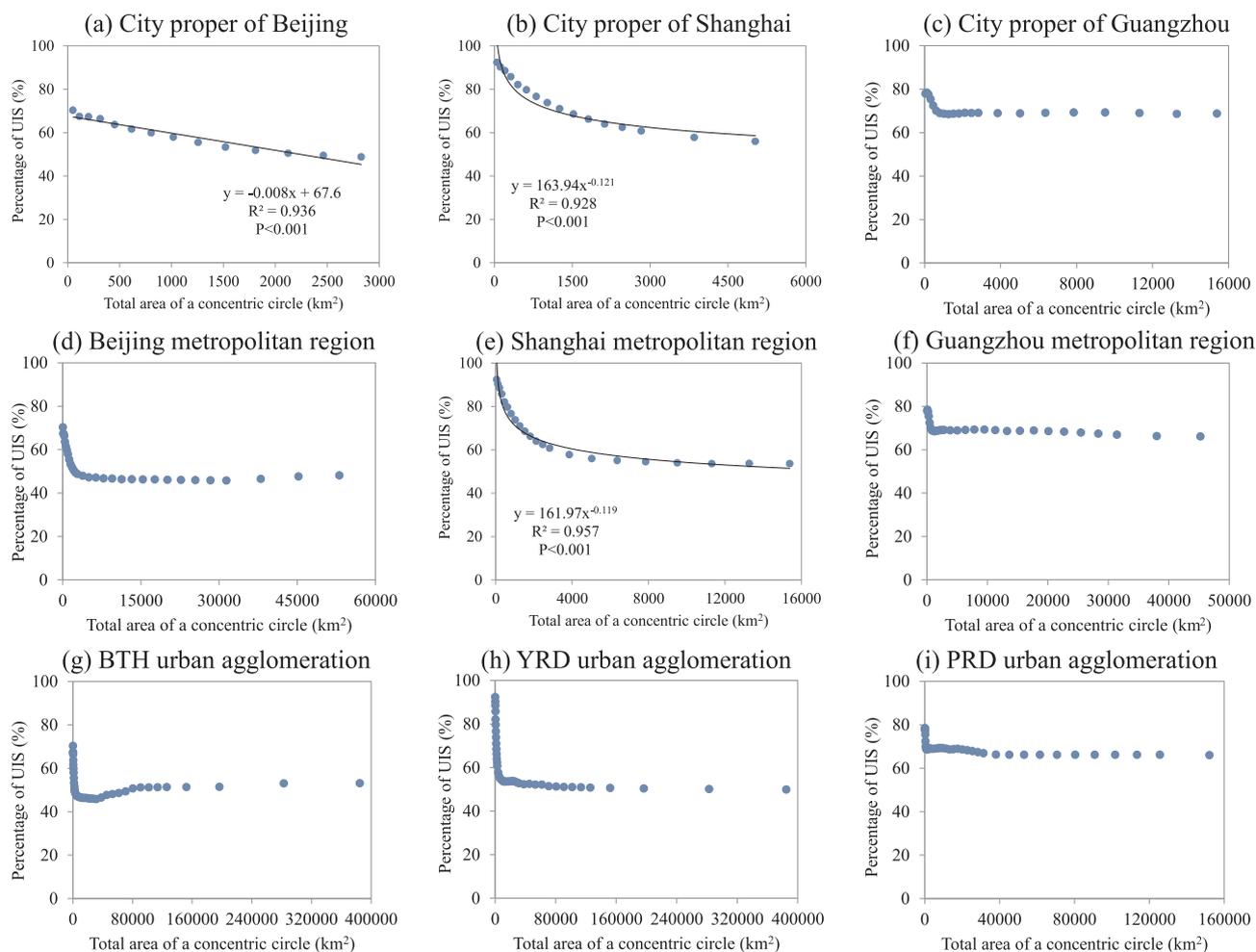
Fig. 4. Scalograms of the percentage of urban impervious surfaces with respect to increasing spatial extent of analysis (represented as the areas of concentric circles) in three major megalopolitan regions of China at the three urban administrative levels: the city proper (a-c), the metropolitan region (d-f), and the urban agglomeration (g-i).

of UIS begins to have little change after the spatial extent extends beyond the metropolitan region level. If an urban region has multiple urban centers that are connected at different degrees, the spatial scaling pattern would be of the second type (e.g., Baltimore). In this case, UIS with different densities are continuously distributed within a relatively large spatial extent, and thus the total area of UIS keeps increasing at a slower speed even beyond the local city and metropolitan region levels. If an urban region has multiple urban centers that are relatively far from each other, the spatial scaling pattern would be of the third type (e.g., Beijing). In this case, the total area of UIS increases a little beyond the local city, but picks up the speed again after another metropolitan region is encountered.

The above discussion is supported by the scalograms of UIS for the six metropolitan regions which show scale breaks that correspond well to the boundaries of their administrative levels. These scale breaks, as well as those in the scalograms of the Chinese urban agglomerations, may further imply that different urban administrative levels (or scale domains) are dominated by different biophysical and socioeconomic controls, thus resulting in different spatial patterns of UIS. This finding of UIS scale multiplicity suggests that curbing the sprawl of UIS or improving the spatial pattern of UIS will require efforts from different levels of urban administrative hierarchy, each of which should have different priorities. For the city proper level, population policies may be key to effective management of UIS, especially in China (Ma, He et al., 2016). For the metropolitan region and urban agglomeration levels, the UIS management should pay more attention to concerted development of demographic, economic, and transportation sectors, so as to optimize

the spatial patterns of UIS and help achieve urban sustainability.

4.3. Can we predict UIS across spatial scales or administrative levels of urban hierarchy?

The answer from our results is yes and no. Predicting UIS within the city proper or between urban hierarchical levels can be done readily with a simple power law function, as our results have shown. However, directly predicting UIS from a local city to an urban agglomeration is probably not feasible because deriving a mathematical equation for the varying staircase-like changes is formidable if not impossible. This means that using one simple scaling function to extrapolate or interpolate UIS across a broad region with multiple administrative levels may lead to unwarranted results. In this case, the scaling-ladder approach is more effective, in which a simple scaling function is used only within the same scale domain defined by scale breaks (Wu, 1999). In our study, such scale domains were readily identifiable by the straight line segments in the log-log scalograms (e.g., Figs. 5 and 6).

Our results also show that UIS was more predictable within the city proper than over the metropolitan region and urban agglomeration, with more variable scaling relations at the higher levels. Also, the scaling relations of the total area of UIS were more consistent and predictable than those of the percentage of UIS at all three administrative levels (Figs. 3–5). This is similar to the previous findings that, with increasing spatial extent of analysis, the total area of a patch type in a landscape is more consistently predictable than the area percentage of that patch type (Wu, 2004). Similarly, the total number of patches in
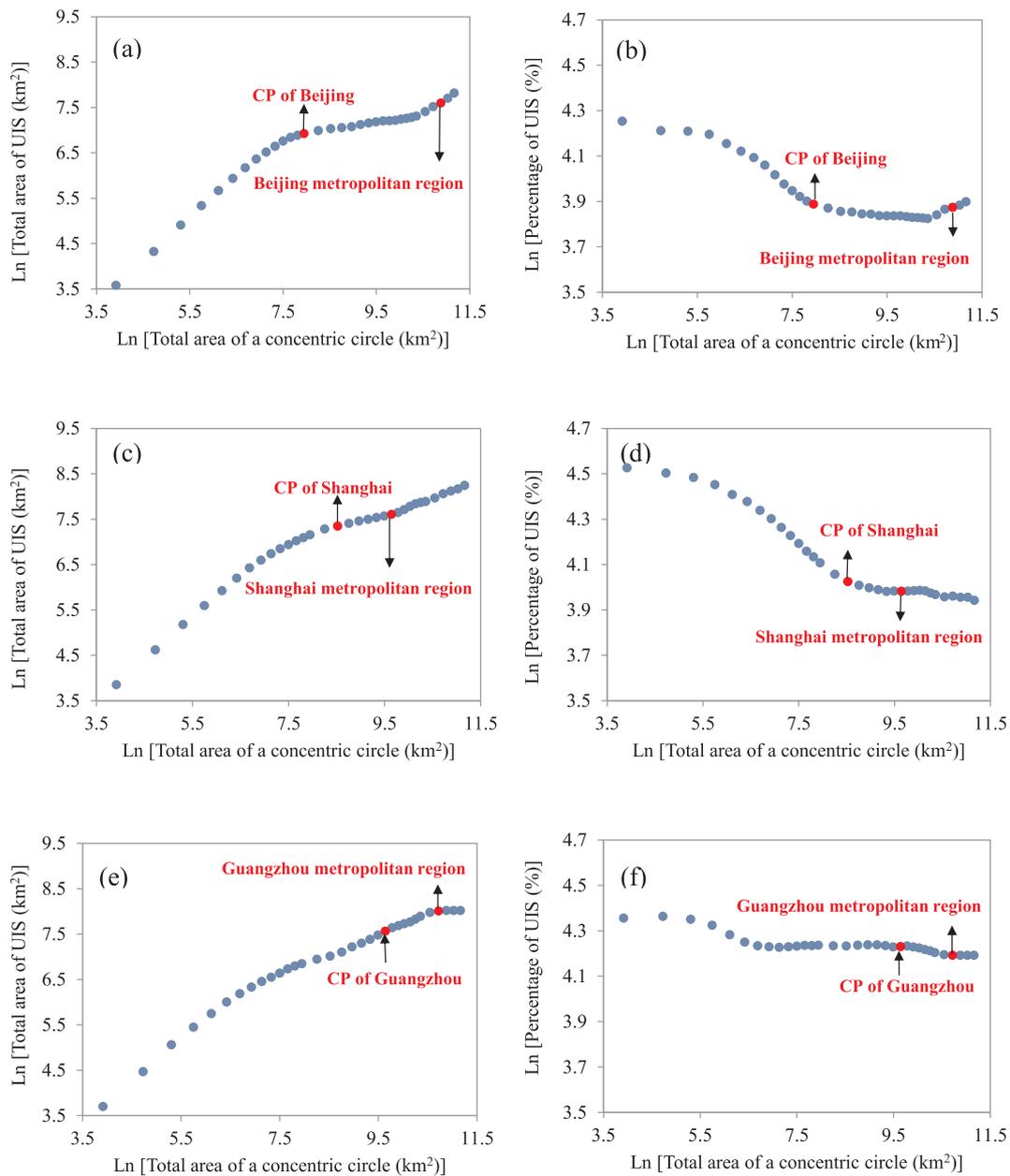
Fig. 5. Log-log plots of the total area and percentage of urban impervious surfaces against spatial extent for Beijing (a-b), Shanghai (c-d), and Guangzhou (e-f). The red dots indicate the locations on the X-axis corresponding to the approximate boundaries that enclose the two urban administrative levels – the city proper and the metropolitan region to assist interpretation. (For interpretation of the references to colour in this figure legend, the reader is referred to the web version of this article.)

a landscape has a much more consistent scaling relation than the patch density of the landscape (Wu, 2004; Wu et al., 2002).

4.4. How does UIS scale with urban population and urban area?

City size-based scaling relations, such as the well-known rank-size distribution (a.k.a. Zipf's law for cities) have long been investigated (Batty, 2008; Bettencourt, 2013; Bettencourt, Lobo, Helbing, Kühnert, & West, 2007; Gabaix, 1999). A number of studies have reported that many properties of cities follow power-law scaling functions, including GDP, total electrical consumption, crimes, gasoline stations, road surface, interactions per capita, wealth creation, and innovation (Bettencourt, 2013; Bettencourt et al., 2007). These are allometric scaling relations of cities which usually use urban population size to represent city size as the independent variable. Although our study focused mainly on the spatial allometry of UIS, in which the spatial extent of urban area is the independent variable, the scaling of UIS with respect to urban population is also of immediate relevance.

Our results show that the total area of UIS had a power-law scaling relation with city size, represented by either urban population size or urban area (Table 2; Fig. 7). The scaling exponent was larger than 1 (superlinearly) with respect to urban area, but smaller than 1 (sublinearly) for urban population size. These results indicate that UIS increased faster than urban area, and the increase rate of UIS accelerated with urban area. This is consistent with the finding by Kuang, Liu, Zhang, Lu, and Xiang (2013) that during 2000–2008 the growth rate of UIS in China (53.30%) were larger than that of China's urban area (43.46%). On the other hand, the urban population-based scaling of UIS indicates that urban population increased more rapidly than the area of UIS, and this was more so as urban population became larger. Our results corroborate the prediction by Bettencourt et al. (2007) that the scaling exponents for urban indicators associated with materials and hard infrastructure, such as gasoline stations and road surfaces, are less than 1, whereas those associated with social interactions, such as
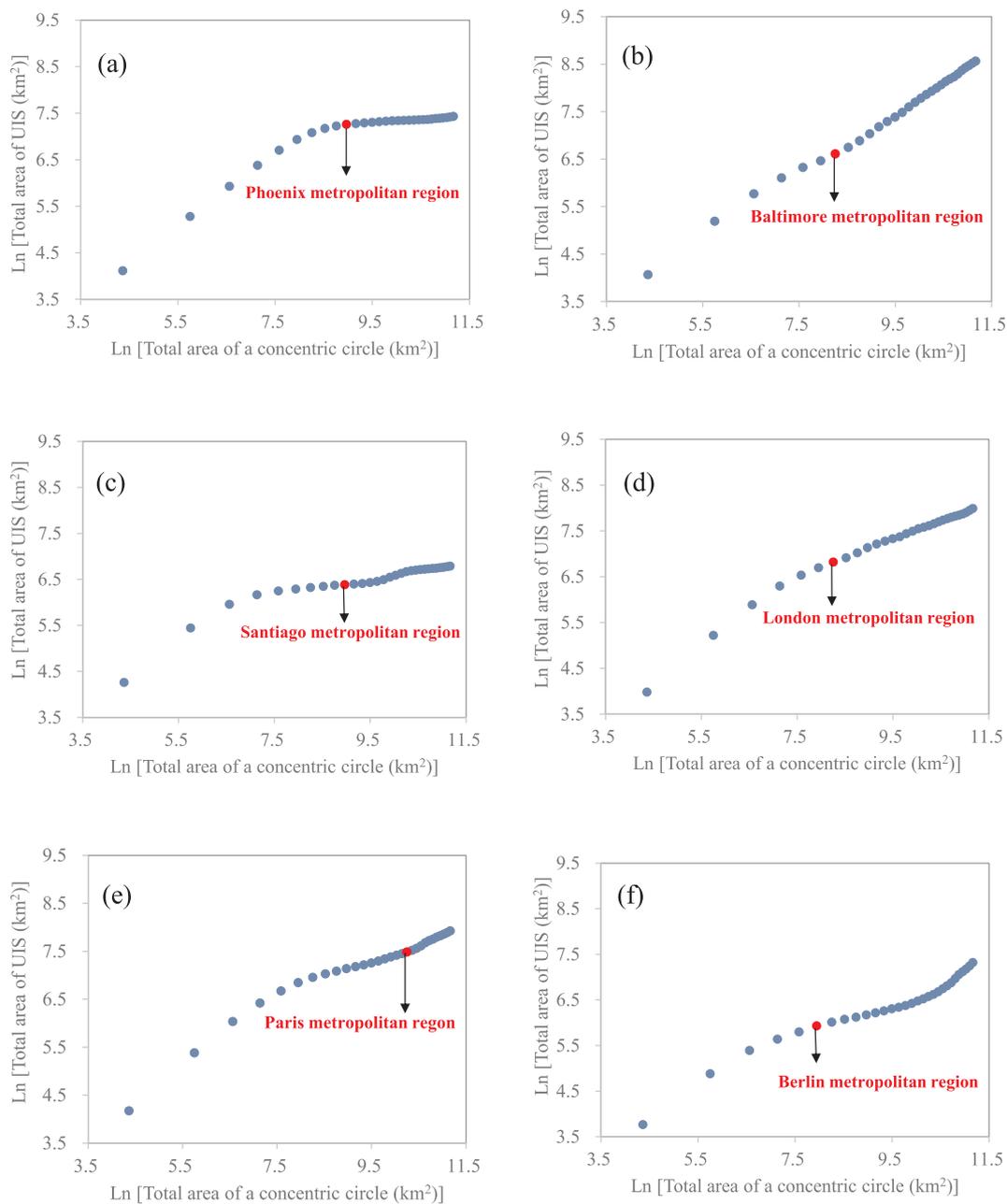
Fig. 6. Log-log plots of the total area of urban impervious surfaces against spatial extent for the six selected world metropolitan regions: Phoenix of the US (a), Baltimore of the US (b), Santiago of Chile (c), London of England (d), Paris of France (e), and Berlin of Germany (f). The red dots indicate the locations on the X-axis corresponding to the boundaries of metropolitan regions to assist interpretation. (For interpretation of the references to colour in this figure legend, the reader is referred to the web version of this article.)

information, innovation, and wealth, are larger than 1. However, Gao, Huang, He, Sun, and Zhang (2016) reported that the annual growth rate of urban areas was 2.45% greater than that of urban population in China during 1990–2010. This is different from our finding probably because we used the ambient population data which more accurately reflect the current population distributions, whereas Gao et al. (2016) used the census data which did not include most ambient populations in transportation networks (e.g., airports and railroads) of a region.

Can urban population be a reliable surrogate for urban area in the spatial scaling of UIS? Our results show that, although the area of UIS scaled both with urban area and urban population size, the scaling relation seemed much tighter for urban area than for urban population size, due to the higher values of coefficient of determination (Fig. 7). This means that using urban area to predict the area of UIS will have a higher accuracy than using urban population size.

5. Conclusions

Several conclusions about the spatial scaling of UIS can be made from our study. First, the total area of UIS increases and the percentage of UIS decreases with spatial extent of analysis from a city center, but these changes exhibit a staircase-like pattern for large regions that contain multiple administrative levels. Second, changes in the total area and percentage of UIS can be predicted with simple scaling functions (e.g., a power law) within a local city or between two adjacent urban hierarchical levels, but not over the entire metropolitan region or urban agglomeration. Third, the scaling relations of UIS generally are more consistent and reliable within single cities than between higher urban hierarchical levels. Fourth, the scaling relations of UIS are more consistent and reliable for the total area of UIS than for the percentage of UIS. Fifth, the amount of UIS scales both with urban area (scaling exponent of larger than 1) and urban population size (scaling exponent of
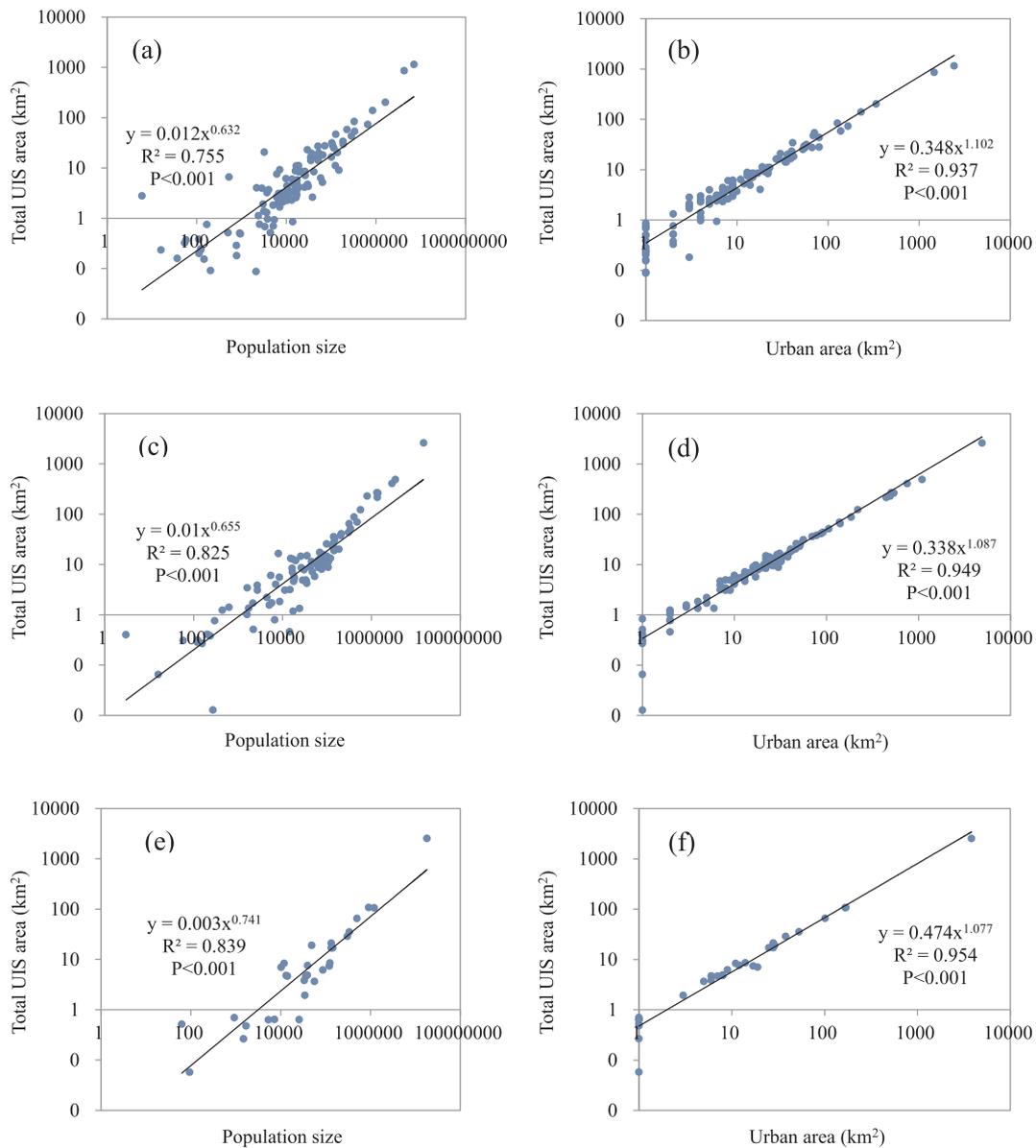
Fig. 7. Scalograms of the total area of urban impervious surfaces against urban population size and urban area in the Beijing-Tianjin-Hebei urban agglomeration (a-b), the Yangtze River Delta urban agglomeration (c-d), and the Pearl River Delta urban agglomeration (e-f).

Table 2
Scaling exponent in the relationship of the total area of UIS with urban population size and urban area in the three major urban agglomerations of China.

Log-log Relationship	Index	BTH	YRD	PRD
UIS-Population size	Scaling exponent	0.728	0.721	0.809
	95% Confidence interval	0.663–0.798	0.664–0.783	0.695–0.942
	R^2	0.755	0.825	0.839
	P-value	< 0.001	< 0.001	< 0.001
	Observations	114	103	31
UIS-Urban area	Scaling exponent	1.139	1.116	1.103
	95% Confidence interval	1.086–1.193	1.067–1.167	1.017–1.197
	R^2	0.937	0.949	0.954
	P-value	< 0.001	< 0.001	< 0.001
	Observations	114	104	31

smaller than 1), but urban area is a more accurate predictor of UIS than urban population size. In addition, the increase rate of UIS is larger than that of urban area, but smaller than that of urban population. These findings together help us better understand and predict how the total amount and percentage of UIS change across space, which is important to the study and improvement of urban environments. Because rapid urbanization is usually associated with fast expansion of UIS, these findings are particularly useful for understanding the processes and consequences of rapidly evolving urban landscapes in developing countries around the world.

Acknowledgments

Appendix A. Supplementary data

Supplementary data associated with this article can be found, in the online version, at http://dx.doi.org/10.1016/j.landurbplan.2018.03.010.

References

Argañaraz, J. P., & Entraigas, I. (2014). Scaling functions evaluation for estimation of landscape metrics at higher resolutions. *Ecological Informatics, 22*, 1–12.

Arnold, C. L., & Gibbons, C. J. (1996). Impervious surface coverage – The emergence of a key environmental indicator. *Journal of the American Planning Association, 62*(2), 243–258.

Batty, M. (2008). The size, scale, and shape of cities. *Science, 319*(5864), 769–771.

Beijing Municipal Bureau of Statistics NBS Survey Office in Beijing (2011). *Beijing statistical yearbook 2011.* Beijing: China Statistics Press (in Chinese).

Bettencourt, L. M. (2013). The origins of scaling in cities. *Science, 340*(6139), 1438–1441.

Bettencourt, L. M., Lobo, J., Helbing, D., Kühnert, C., & West, G. B. (2007). Growth, innovation, scaling, and the pace of life in cities. *Proceedings of the National Academy of Sciences, 104*(17), 7301–7306.

Brabec, E. (2002). Impervious surfaces and water quality: A review of current literature and its implications for watershed planning. *Journal of Planning Literature, 16*(4), 499–514.

Brun, S., & Band, L. (2000). Simulating runoff behavior in an urbanizing watershed. *Computers, Environment and Urban Systems, 24*(1), 5–22.

Buyantuyev, A., & Wu, J. (2010). Urban heat islands and landscape heterogeneity: Linking spatiotemporal variations in surface temperatures to land-cover and socioeconomic patterns. *Landscape Ecology, 25*(1), 17–33.

Department of Urban Surveys of National Bureau of Statistics of China (2011). *China city statistics yearbook 2009.* Beijing: China Statistics Press (in Chinese).

Dobson, J. E., Bright, E. A., Coleman, P. R., Durfee, R. C., & Worley, B. A. (2000). LandScan: A global population database for estimating populations at risk. *Photogrammetric Engineering and Remote Sensing, 66*(7), 849–857.

Elvidge, C. D., Tuttle, B. T., Sutton, P. S., Baugh, K. E., Howard, A. T., Milesi, C., et al. (2007). Global distribution and density of constructed impervious surfaces. *Sensors, 7*(9), 1962–1979.

Fang, C. (2011). New structure and new trend of formation and development of urban agglomerations in China. *Scientia Geographica Sinica, 31*(9), 1025–1034.

Fang, C. (2015). Important progress and future direction of studies on China's urban agglomerations. *Journal of Geographical Sciences, 25*(8), 1003–1024.

Forman, R. T. (2016). Urban ecology principles: Are urban ecology and natural area ecology really different? *Landscape Ecology, 31*(8), 1653–1662.

Frazier, A. E. (2016). Surface metrics: Scaling relationships and downscaling behavior. *Landscape Ecology, 31*(2), 351–363.

Frohn, R. C., & Hao, Y. (2006). Landscape metric performance in analyzing two decades of deforestation in the Amazon Basin of Rondonia, Brazil. *Remote Sensing of Environment, 100*(2), 237–251.

Fuller, R. A., & Gaston, K. J. (2009). The scaling of green space coverage in European cities. *Biology Letters, 5*(3), 352–355.

Gabaix, X. (1999). Zipf's law for cities: An explanation. *Quarterly Journal of Economics, 114*(3), 739–767.

Gao, B., Huang, Q., He, C., Sun, Z., & Zhang, D. (2016). How does sprawl differ across cities in China? A multi-scale investigation using nighttime light and census data. *Landscape and Urban Planning, 148*(41), 89–98.

Goetz, S., & Fiske, G. (2008). Linking the diversity and abundance of stream biota to landscapes in the mid-Atlantic USA. *Remote Sensing of Environment, 112*(11), 4075–4085.

Grimm, N. B., Faeth, S. H., Golubiewski, N. E., Redman, C. L., Wu, J., Bai, X., et al. (2008). Global change and the ecology of cities. *Science, 319*(5864) 756-60.

Jelinski, D. E., & Wu, J. (1996). The modifiable areal unit problem and implications for landscape ecology. *Landscape Ecology, 11*(3), 129–140.

Kuang, W., Chi, W., Lu, D., & Dou, Y. (2014). A comparative analysis of megacity expansions in China and the US: Patterns, rates and driving forces. *Landscape and Urban Planning, 132*, 121–135.

Kuang, W., Liu, J., Zhang, Z., Lu, D., & Xiang, B. (2013). Spatiotemporal dynamics of impervious surface areas across China during the early 21st century. *Chinese Science Bulletin, 58*(14), 1691–1701.

Levin, S. A. (1992). The problem of pattern and scale in ecology: The Robert H. MacArthur award lecture. *Ecology, 73*(6), 1943–1967.

Li, H., Han, X., & Wu, J. (2006). Variant scaling relationship for mass-density across tree-dominated communities. *Journal of Integrative Plant Biology, 48*(3), 268–277.

Li, C., Li, J., & Wu, J. (2013). Quantifying the speed, growth modes, and landscape pattern changes of urbanization: A hierarchical patch dynamics approach. *Landscape Ecology, 28*(10), 1875–1888.

Liu, Z., He, C., & Wu, J. (2016). General spatiotemporal patterns of urbanization: An examination of 16 World cities. *Sustainability, 8*(41), 1–15.

Liu, Z., He, C., Zhou, Y., & Wu, J. (2014). How much of the world's land has been urbanized, really? A hierarchical framework for avoiding confusion. *Landscape Ecology, 29*(5), 763–771.

Lu, D., Li, G., Kuang, W., & Moran, E. (2014). Methods to extract impervious surface areas from satellite images. *International Journal of Digital Earth, 7*(2), 93–112.

Luck, M. A., Jenerette, G. D., Wu, J., & Grimm, N. B. (2001). The urban funnel model and the spatially heterogeneous ecological footprint. *Ecosystems, 4*(8), 782–796.

Ma, Q., He, C., & Wu, J. (2016). Behind the rapid expansion of urban impervious surfaces in China: Major influencing factors revealed by a hierarchical multiscale analysis. *Land Use Policy, 59*, 434–445.

Ma, Q., He, C., Wu, J., Liu, Z., Zhang, Q., & Sun, Z. (2014). Quantifying spatiotemporal patterns of urban impervious surfaces in China: An improved assessment using nighttime light data. *Landscape and Urban Planning, 130*, 36–49.

Ma, Q., Wu, J., & He, C. (2016). A hierarchical analysis of the relationship between urban impervious surfaces and land surface temperatures: Spatial scale dependence, temporal variations, and bioclimatic modulation. *Landscape Ecology, 31*(5), 1139–1153.

Oke, T. R. (1982). The energetic basis of the urban heat island. *Quarterly Journal of the Royal Meteorological Society, 108*(455), 1–24.

Population Census Office under the State Council & Department of Population and Employment Statistics of National Bureau of Statistics of China (2013). *Tabulation on the 2010 population census of China.* Beijing: China Statistics Press (in Chinese).

Potere, D., & Schneider, A. (2007). A critical look at representations of urban areas in global maps. *GeoJournal, 69*(1–2), 55–80.

Saura, S. (2004). Effects of remote sensor spatial resolution and data aggregation on selected fragmentation indices. *Landscape Ecology, 19*(2), 197–209.

Saura, S., & Castro, S. (2007). Scaling functions for landscape pattern metrics derived from remotely sensed data: Are their subpixel estimates really accurate? *ISPRS Journal of Photogrammetry and Remote sensing, 62*(3), 201–216.

Shen, W., Darrel Jenerette, G., Wu, J., & Gardner, R. H. (2004). Evaluating empirical scaling relations of pattern metrics with simulated landscapes. *Ecography, 27*(4), 459–469.

State Council of the People's Republic of China (2014). National New-type Urbanization Plan (2014–2020). (in Chinese).

Wang, L., Li, C., Ying, Q., Cheng, X., Wang, X., Li, X., et al. (2012). China's urban expansion from 1990 to 2010 determined with satellite remote sensing. *Chinese Science Bulletin, 1*–11.

Warton, D. I., Wright, I. J., Falster, D. S., & Westoby, M. (2006). Bivariate line-fitting methods for allometry. *Biological Reviews, 81*(2), 259–291.

Weng, Q. (2001). Modeling urban growth effects on surface runoff with the integration of remote sensing and GIS. *Environmental Management, 28*(6), 737–748.

Weng, Q. (2012). Remote sensing of impervious surfaces in the urban areas: Requirements, methods, and trends. *Remote Sensing of Environment, 117*, 34–49.

Wiens, J. A. (1989). Spatial scaling in ecology. *Functional Ecology, 3*(4), 385–397.

Wu, J. (1999). Hierarchy and scaling: Extrapolating information along a scaling ladder. *Canadian Journal of Remote Sensing, 25*(4), 367–380.

Wu, J. (2004). Effects of changing scale on landscape pattern analysis: Scaling relations. *Landscape Ecology, 19*(2), 125–138.

Wu, J. (2014). Urban ecology and sustainability: The state-of-the-science and future directions. *Landscape and Urban Planning, 125*, 209–221.

Wu, J., & David, J. L. (2002). A spatially explicit hierarchical approach to modeling complex ecological systems: Theory and applications. *Ecological Modelling, 153*(1), 7–26.

Wu, J., Bruce Jones, K., Li, H., & Loucks, O. L. (2006). *Scaling and uncertainty analysis in ecology: Methods and applications.* The Netherlands: Springer, Dordrecht.

Wu, J., Gao, W., & Tueller, P. T. (1997). Effects of changing spatial scale on the results of statistical analysis with landscape data: A case study. *Geographic Information Sciences, 3*(1–2), 30–41.

Wu, J., Jelinski, D. E., Luck, M., & Tueller, P. T. (2000). Multiscale analysis of landscape heterogeneity: Scale variance and pattern metrics. *Geographic Information Sciences, 6*(1), 6–19.

Wu, J., & Li, H. (2006). Perspectives and methods of scaling. In J. Wu, B. Jones, H. Li, & O. L. Loucks (Eds.). *Scaling and uncertainty analysis in ecology* (pp. 17–44). Dordrecht, The Netherlands: Springer.

Wu, J., Shen, W., Sun, W., & Tueller, P. T. (2002). Empirical patterns of the effects of changing scale on landscape metrics. *Landscape Ecology, 17*(8), 761–782.

Wu, J., Xiang, W.-N., & Zhao, J. (2014). Urban ecology in China: Historical developments and future directions. *Landscape and Urban Planning, 125*, 222–233.

Zhou, Y., Smith, S. J., Zhao, K., Imhoff, M., Thomson, A., Bond-Lamberty, B., et al. (2015). A global map of urban extent from nightlights. *Environmental Research Letters, 10*(5), 054011.